Supplementary Information: Subtle Changes in pH Affect the Packing and Robustness of Fatty Acid Bilayers

Lauren A. Lowe, James T. Kindt, Charles Cranfield, Bruce Cornell, Alexander Macmillan, and Anna Wang*
*anna.wang@unsw.edu.au

Molecular Dynamics Simulations

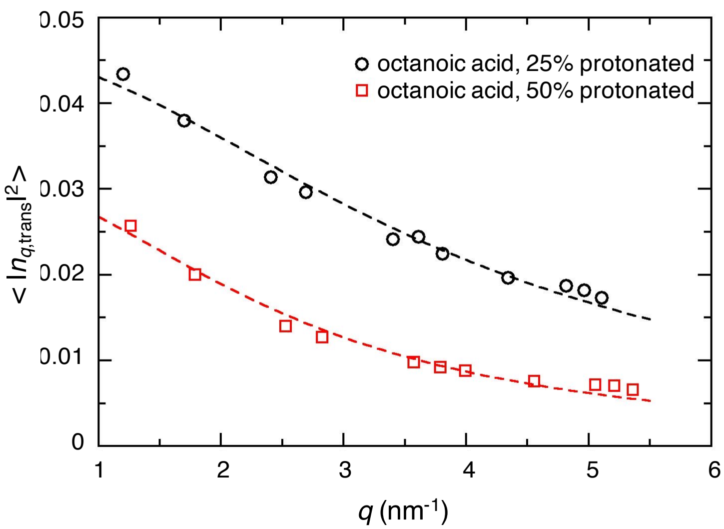

Figure S1: Mean square Fourier components of transverse fluctuations, indicating molecular tilt, and fits to Equation 5 in the main text, also shown below. Only data up to $q = 5.5$ nm^{-1} were used in the fit made, as we find that the fluctuations do not approach zero at high q as Equation 5 in the main text would predict; molecular-level granular effects are likely responsible.

Equation 4 from main text: $\langle \left|\hat{n}_q^{\parallel}\right|^2 \rangle = \frac{k_B T}{K_\theta + K_{\mathrm{tw}} q^2}$

Lipid Packing

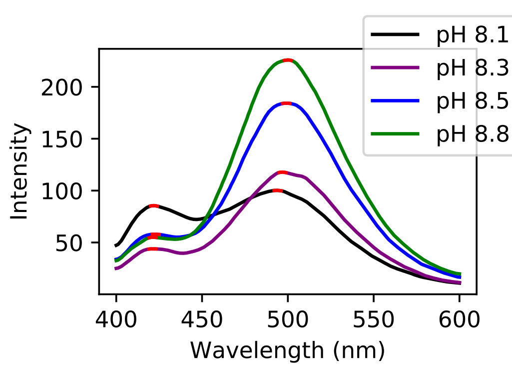

Figure S2: Fluorescence spectra of Laurdan and oleic acid vesicles at varying pH. Red regions indicate the maximum intensities for each peak.

Electrical Impedance Spectroscopy

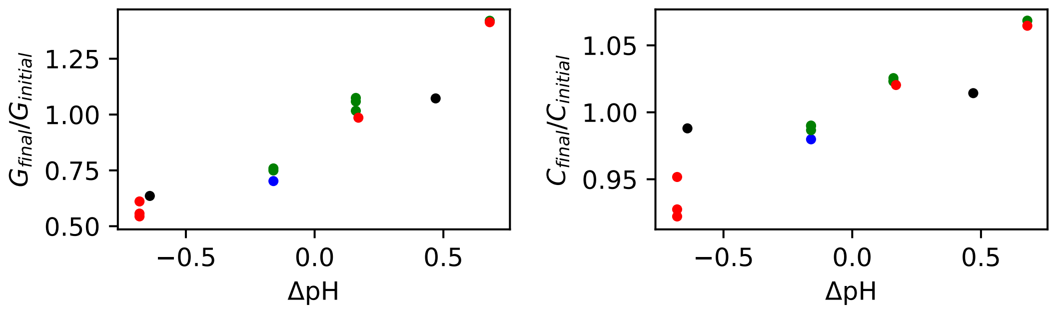

Figure S3: AC impedance spectroscopy performed on oleic acid tBLMs at varying pHs. Relative conductance and capacitance across tBLMs increases with an increase in pH. Colours represent different trials.

A trial (separate colours in Fig. S3) indicates the use of a different slide and cartridge. We observed some variation in the absolute value of the G and C across cartridges, but not their relative values. This variance is possibly due to differences in the quality of the tethered bilayers formed throughout the different experiments. When tBLMs did not successfully form, indicated by fluctuating or extremely high conductance readings indicative of patchy tBLM formation, the data was not included.

Permeability to Pyranine

The permeability of fatty acid bilayers to pyranine was monitored by preparing 10 mM oleic acid GUVs encapsulating 500 mM sucrose and 1 mM pyranine at pH 8.2 (see Methods) and diluting them 1 in 10 into a buffer containing 500 mM glucose. This pH was chosen because GUVs assemble in high yield. The pH of the dilution buffer was then varied to determine the effect of pH on pyranine. The concentration of sugar inside and outside of the vesicles was matched to prevent the build up of osmotic pressure, potentially leading to vesicle rupture or growth. To monitor pyranine leakage, the vesicles were imaged using fluorescence microscopy over multiple days and the mean intensity of an approximately 1.5 x 1.5 μm square inside (I_{in}) and outside a vesicle (I_{out}) was measured using Fiji (Fig. S4. The normalised vesicle intensity was calculated as follows:

$$\text{Normalised Intensity} = I_{in} - I_{out} I_{out} \tag{1}$$

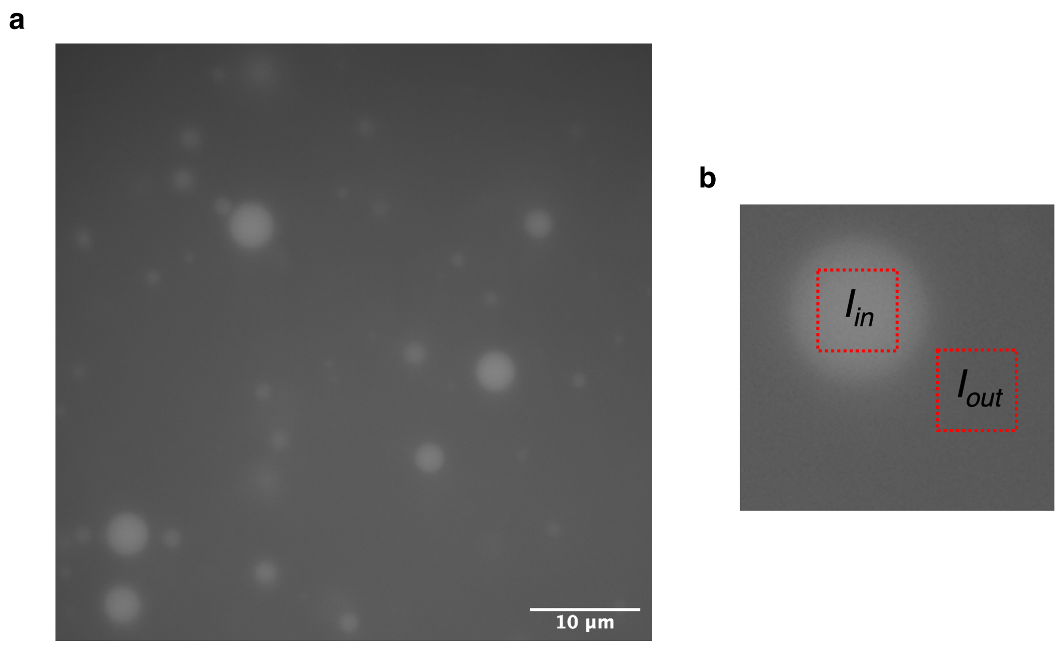

Figure S4: (a) Epifluorescence microscopy image of oleic acid vesicles encapsulating pyranine. (b) Epifluorescence microscopy image showing regions of interest for intensity analysis, I_{in} represents the intensity inside the vesicle, I_{out} represents the intensity outside the vesicle, or the intensity of the background.

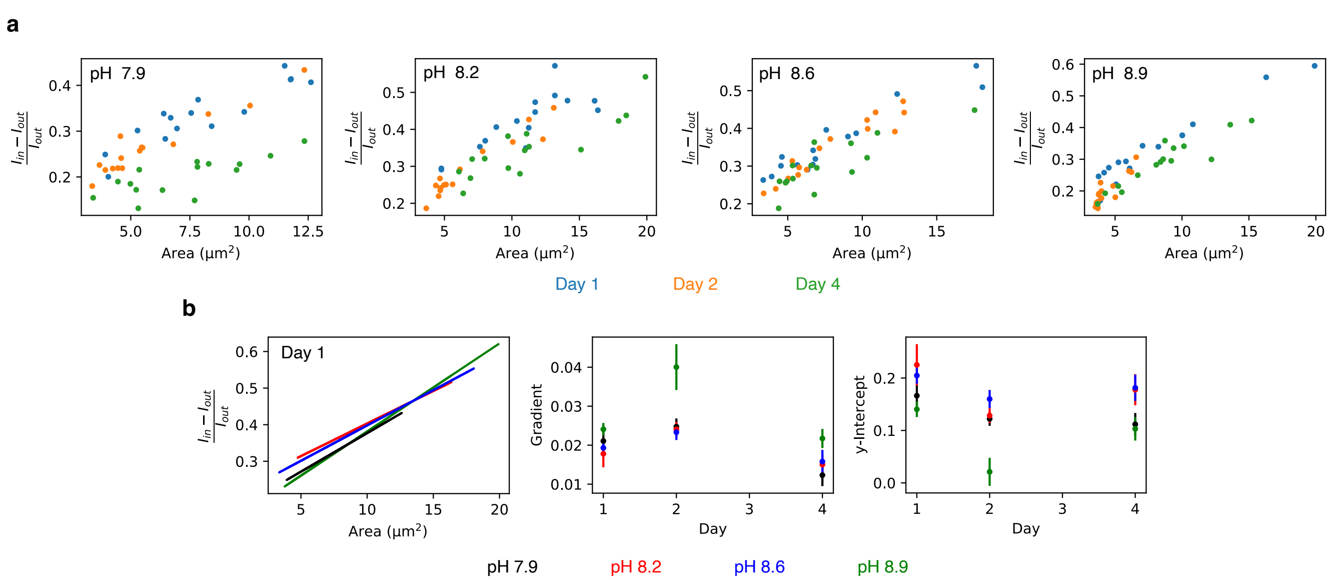

Figure S5: (a) Normalised vesicle intensity vs vesicle area. Vesicle area measured using Fiji by thresholding the image using the Phansalkar auto local threshold and the Analyse Particles tool. Only vesicles in focus and smaller than 20 μm^2 were selected for analysis (n $>$ 15 for each data series). (b) For each pH and time point, the normalised intensity vs area was fit to a straight line (example shown for Day 1) and the gradient and y-intercept plotted. Error bars represent the errors from the line of best fit.

Rupture Tension

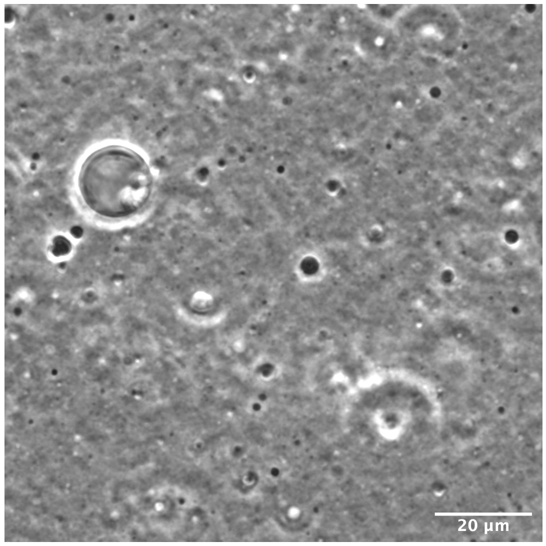

Figure S6: Phase contrast microscopy image of pH 8.4 10 mM oleic acid MLVs encapsulating 100 mM sucrose. Image taken prior to sample extrusion.